NASA Technical Memorandum 107686
ICASE Report No. 92–50

ICASE

HOMOGENEOUS QUANTUM ELECTRODYNAMIC TURBULENCE

John V. Shebalin

October 1992

Institute for Computer Applications in Science and Engineering
NASA Langley Research Center
Hampton, Virginia 23681–0001

Operated by the Universities Space Research Association

National Aeronautics and
Space Administration

Langley Research Center
Hampton, Virginia 23665-5225

HOMOGENEOUS QUANTUM ELECTRODYNAMIC TURBULENCE

John V. Shebalin[1]

National Aeronautics and Space Administration

Langley Research Center

Hampton, VA 23681, USA

The electromagnetic field equations and Dirac equations for oppositely charged wave functions are numerically time-integrated using a spatial Fourier method. The numerical approach used, a spectral transform technique, is based on a continuum representation of physical space. The coupled classical field equations contain a dimensionless parameter which sets the strength of the nonlinear interaction (as the parameter increases, interaction volume decreases). For a parameter value of unity, highly nonlinear behavior in the time-evolution of an individual wave function, analogous to ideal fluid turbulence, is observed. In the truncated Fourier representation which is numerically implemented here, the quantum turbulence is homogeneous but anisotropic and manifests itself in the nonlinear evolution of equilibrium modal spatial spectra for the probability density of each particle and also for the electromagnetic energy density. The results show that nonlinearly interacting fermionic wave functions quickly approach a multi-mode, dynamic equilibrium state, and that this state can be determined by numerical means.

[1]Research supported by the National Aeronautics and Space Adminstration. The author is currently in residence as a Visiting Scientist at the Institute for Computer Applications in Science and Engineering (ICASE), NASA Langley Research Center, Hampton, VA 23681.

1. Introduction

A direct numerical simulation of the self-consistent electromagnetic interaction between two oppositely charged and densely packed spin 1/2 Dirac particles is presented here. While the approach taken here is nonperturbative, it is not based on lattice gauge theory. Instead, it is a solution of the basic set of coupled, nonlinear partial differential equations which describe a fundamental quantum mechanical system in terms of classical field theory. These equations are integrated forward in time to simulate the nonlinear evolution of two Dirac wave functions and the electromagnetic field which couples them.

The means of solution is a Fourier spectral method, in which a three-dimensional momentum space (**k**-space) is restricted to contain only a finite number of discrete modes (*i.e.*, $|\mathbf{k}| \leq k_{max}$). Although **k**-space is discretized, position space (**x**-space) is not: The underlying physical space is a *continuum* and not a discrete set of points. The Fourier spectral method has been used to great advantage in pioneering work in turbulent flow simulation [1] and continues to be used in the study of turbulence and other nonlinear dynamic phenomena.

Since the interaction of strongly coupled fields is essentially nonlinear, it is generally not possible to assign a specific frequency to each spatial mode. The actual time dependence of the Fourier modes is found by integrating the equations of motion, after which a time sequence for each mode may be analyzed to determine its frequency content during the sampling time. However, it must be remembered that in the evoultion of a nonlinear dynamic system the frequency content of a mode is constantly changing, as the various modes are nonlinearly interacting with one another. To robustly determine the frequency spectrum for any mode requires that a simulation be run considerably past the time at which the initial conditions are 'forgotten' by the nonlinear system. That is computationally expensive (for a large number of grid points) and will not be done here, although the simulation will be run long enough to see the establishment of spatial equilibria for the interacting wave functions.

Strongly interacting quantum mechanical wave fields can exhibit the same interesting nonlinear dynamic behavior seen in fluids and plasmas, *i.e.*, chaos and turbulence. (Chaos and turbulence are related in that turbulence may be thought of as many degree-of-freedom chaotic motion, while "classical" chaos appears, for example, when the mathematical model of a turbulent hydrodynamic system is reduced to a minimum number of degrees-of-freedom [2].) Here, the continuous wave functions and electromagnetic field play a role similar to that of conserved components in a mixture of classical fluids; for example, probability densities are analogous to component mass densities as both satisfy identical continuity equations. Turbulent behavior will be seen in the dynamic transfer of energy and probability between different spatial modes and in the establishment of apparent equilibrium modal spatial spectra.

Again, it is the electromagnetic interaction of oppositely charged spin-1/2 particles (an "electron" and a "positron") which we examine here. This classical "lepton-photon" system is described by Dirac equations and the electromagnetic field equations. Although replacing the Dirac equations with Schrödinger equations also produces a system which contains the nonlinear electromagnetic interaction, the coupling parameter is small and the nonlinear interaction is weak. The coupling parameter will be seen to increase as the density of particles increases; concomitantly, the mean particle velocity will become more and more relativistic. Thus, the description of a lepton-photon (or any fermion-gauge field) system with a strong nonlinear interaction requires the use of the Dirac equation, rather than the Schrödinger equation.

In this paper a first-quantized or "classical" field description will be utilized, which will allow us to follow the self-consistent evolution of the oppositely charged, two particle quantum mechanical system. The basic equations will be given in nondimensional form, followed by the classical Noether invariants of the system. Then the numerical method will be described, and numerical results will be presented.

In addition to observing turbulence in a quantum mechanical system, the novelty of the work presented here is that it introduces a new, nonperturpative and direct approach to studying the gauge field interaction of closely packed particles, such as those in extremely dense matter. The current historical context is similar to that encountered when time-integration methods on a spatial grid were introduced into the study of general relativistic flow problems [3] and into nonrelativistic quantum processes [4], *i.e.*, although previous analytical and numerical techniques have produced and continue to produce many valuable results, time integration methods allow the problem at hand to be solved (and visualized) directly.

A study of coupled nonlinear Dirac equations in four dimensions has appeared before, in the work of Alvarez [5], where soliton-like behavior was examined. In that work, however, the mediating gauge field was eliminated by introducing *ad hoc* terms into two separate free-particle Dirac equations so as to produce a direct nonlinear coupling. Here, we study two classical Dirac fields realistically coupled by an electromagnetic field and, in this case, do not find the 'blow-up' problem which appears in the direct nonlinear coupling model [6]. The approach taken here is also generically similary to that of Bialynicki-Birula, *et al.*, who have recently examined the self-consistent time evolution of quantum fields in terms of the Wigner distribution function [7].

2. Basic Equations

The Dirac equation is (here, standard notation [8] is used)

$$\gamma^{\mu}(p_{\mu}-\frac{e}{c}A_{\mu})\Psi = mc\Psi, \qquad p_{\mu} \equiv i\frac{h}{2\pi}\partial_{\mu}. \tag{1}$$

For electrons, e is the negative electronic charge and for positrons, e is the positive electronic charge; m is the electron or positron mass, c is the speed of light, and h is Planck's constant. Explicitly, the (4x4) Dirac matrices are

$$\gamma^0 = \beta, \quad \gamma = \beta\alpha, \qquad \beta \equiv \begin{bmatrix} I & 0 \\ 0 & -I \end{bmatrix}, \quad \alpha \equiv \begin{bmatrix} 0 & \sigma \\ \sigma & 0 \end{bmatrix},$$

$$I = \begin{bmatrix} 1 & 0 \\ 0 & 1 \end{bmatrix}, \quad \sigma_x = \begin{bmatrix} 0 & 1 \\ 1 & 0 \end{bmatrix}, \quad \sigma_y = \begin{bmatrix} 0 & -i \\ i & 0 \end{bmatrix}, \quad \sigma_z = \begin{bmatrix} 1 & 0 \\ 0 & -1 \end{bmatrix}, \tag{2}$$

(Greek indices range from 0 to 3 with a metric signature of +---, while Latin indices range over 1, 2, 3 (*i. e.*, x, y, z) with a metric signature of +++; repeated indices imply summation. Also, boldface denotes a 3-vector.)

The electron and positron wave functions are complex entities and will be expressed here as

$$\Psi_e = R + iS = \begin{bmatrix} R_1 \\ R_2 \\ R_3 \\ R_4 \end{bmatrix} + i\begin{bmatrix} S_1 \\ S_2 \\ S_3 \\ S_4 \end{bmatrix}, \qquad \Psi_p = P + iQ = \begin{bmatrix} P_1 \\ P_2 \\ P_3 \\ P_4 \end{bmatrix} + i\begin{bmatrix} Q_1 \\ Q_2 \\ Q_3 \\ Q_4 \end{bmatrix} \tag{3}$$

where the R_i, S_i, P_i, and Q_i (i=1,2,3,4) are real functions of time and position. Coupled with the Dirac wave equations are the electromagnetic field equations (using the Lorentz gauge condition):

$$\left(\partial_t^2 - \nabla^2\right) A^\mu = |e|\, j^\mu = |e|\left(j_e^\mu - j_p^\mu\right), \qquad \partial_\mu A^\mu = 0$$
$$j_e^\mu \equiv \overline{\Psi}_e \gamma^\mu \Psi_e, \qquad j_p^\mu \equiv \overline{\Psi}_p \gamma^\mu \Psi_p, \qquad \overline{\Psi} \equiv \Psi^{*T} \gamma^0 \tag{4}$$

The conservation of probability is guaranteed by the continuity equations each wave function satisfies: $\partial_\mu j^\mu = \partial_t \rho + \nabla \cdot \mathbf{j} = 0$, where $j^\mu = (\rho, \mathbf{j})$ corresponds to either particle.

At this point, we will nondimensionalize equations (1) and (4). Since a spatial Fourier method will presently be used for numerical simulation, units of distance will be in terms of $L_o / 2\pi$, where L_o is the side length of the periodic physical cube. Using the operator equivalence given in (1), the nonlinearly coupled, nondimensional dynamic equations are

$$\gamma^\mu\left(\partial_\mu + iA_\mu\right)\Psi_e = -i\Psi_e, \qquad \gamma^\mu\left(\partial_\mu - iA_\mu\right)\Psi_p = -i\Psi_p$$
$$\left(\partial_t^2 - \nabla^2\right) A^\mu = \kappa\left(j_e^\mu - j_p^\mu\right), \qquad \partial_\mu A^\mu = 0 \tag{5}$$

These equations contain only one parameter which determines the nature of the interaction:

$$\kappa \equiv \alpha\left(\frac{\lambda_c}{L_o}\right)^3 \tag{6}$$

where the Compton wavelength of the electron is $\lambda_c = h/mc = 2.43$ pm and the fine-structure constant is $\alpha = 2\pi e^2/hc = 1/137$. Here, Ψ_s (s=e,p) is normalized so that the integral of j_s^0 over the characteristic volume L_o^3 is equal to unity Note that for the interaction parameter to have a value of unity ($\kappa = 1$), then $L_o = \alpha^{1/3}\lambda_c = 0.47$ pm and the density of particles must be around $L_o^{-3} = 10^{31}$ cm^{-3}; electrons at densities up to 10^{37} cm^{-3} are believed to exist in the outer layers of neutron stars [9]. This density is also achieved by scattering particles whose 'interaction time' is at least 10^{-21} seconds, *i.e.*, 'resonant' particles.

3. Noether Invariants

The classical invariants [10] of the electromagnetically interacting electron-positron system can be derived from the Lagrangian density

$$\Lambda = \frac{i}{2}\left[\overline{\Psi}_e\gamma^\mu\left(D_\mu\Psi_e\right) - \left(D_\mu^*\overline{\Psi}_e\right)\gamma^\mu\Psi_e + \overline{\Psi}_p\gamma^\mu\left(D_\mu^*\Psi_p\right) - \left(D_\mu\overline{\Psi}_p\right)\gamma^\mu\Psi_p\right]$$
$$- \overline{\Psi}_e\Psi_e - \overline{\Psi}_p\Psi_p - \frac{1}{4}F_{\mu\nu}F^{\mu\nu} \qquad (7)$$

where the "covariant" derivative D_μ and the electromagnetic field tensor $F_{\mu\nu}$ are, respectively,

$$D_\mu \equiv \partial_\mu + iA_\mu, \qquad F_{\mu\nu} \equiv \partial_\mu A_\nu - \partial_\nu A_\mu.$$

The nondimensional volume of the 3-space cube is $(2\pi)^3$; an integral over this volume is

$$\langle Q\rangle \equiv \int_v Q(t,\mathbf{r})d\mathbf{r}$$

a definition which allows for notational conciseness. Using Noether's theory [10] (along with $\kappa = 1$), the important classical invariants are found to be

Normalization (total probability):

$$N_e = \langle j_e^o\rangle \equiv \left\langle\overline{\Psi}_e\gamma^o\Psi_e\right\rangle \qquad N_p = \langle j_p^o\rangle \equiv \left\langle\overline{\Psi}_p\gamma^o\Psi_p\right\rangle \qquad (8)$$

Energy:

$$E = \left\langle -i\overline{\Psi}_e\gamma\cdot\nabla\,\Psi_e - i\overline{\Psi}_p\gamma\cdot\nabla\,\Psi_p + \overline{\Psi}_e\Psi_e + \overline{\Psi}_p\Psi_p - \mathbf{A}\cdot(\mathbf{j}_e-\mathbf{j}_p) + \tfrac{1}{2}\left(|\mathbf{E}|^2+|\mathbf{H}|^2\right)\right\rangle$$

$$\left(\mathbf{E} \equiv -\partial_t\mathbf{A} - \nabla A^o,\quad \mathbf{H}\equiv\nabla\times\mathbf{A},\quad \mathbf{j}_e\equiv\overline{\Psi}_e\gamma\Psi_e,\quad \mathbf{j}_p\equiv\overline{\Psi}_p\gamma\Psi_p\right) \tag{9}$$

Momentum:

$$\mathbf{P} = \langle\mathbf{p}\rangle \equiv \left\langle -i\overline{\Psi}_e\gamma^o\nabla\,\Psi_e - i\overline{\Psi}_p\gamma^o\nabla\,\Psi_p + \mathbf{A}\left(j_p^o - j_e^o\right) + \mathbf{E}\times\mathbf{H}\right\rangle \tag{10}$$

Angular Momentum:

$$\mathbf{J} = \left\langle \mathbf{r}\times\mathbf{p} + \tfrac{1}{2}\overline{\Psi}_e\gamma^o\Sigma\,\Psi_e + \tfrac{1}{2}\overline{\Psi}_p\gamma^o\Sigma\,\Psi_p + \mathbf{A}\times\partial_t\mathbf{A}\right\rangle, \qquad \Sigma \equiv \begin{bmatrix}\sigma & 0\\ 0 & \sigma\end{bmatrix} \tag{11}$$

The invariants (8) through (11) are classical and the fields contained in them are not considered to consist of explicit creation and annihilation operators [10]; according to the tenets of Lagrangian field theory, these invariants should be preserved during the time-evolution of a closed system. The invariance of a numerical model based on equations (5) will be examined in the next section. (The specific parts of these invariants which are associated with either the electron, positron, or photon fields, or with their interaction, can be easily separated out of the total expression and examined individually, as required.)

4. Numerical Results

Using the equations given in (5), the time-evolution of the lepton-photon system was simulated on a 32x32x32 **k**-space grid. Simulations were performed using a spatial Fourier transform method [11] with a de-aliased [12], third-order time-integration scheme [13] (this approach is somewhat similar to that used in nonrelativistic quantum mechanics simulations [14]). For numerical simulation, the equations (5) are expressed as follows:

$$\partial_t \Psi_e = -\left[\alpha\cdot\nabla + i\left(\beta + \varphi - \alpha\cdot\mathbf{A}\right)\right]\Psi_e, \qquad \partial_t \Psi_p = -\left[\alpha\cdot\nabla + i\left(\beta - \varphi + \alpha\cdot\mathbf{A}\right)\right]\Psi_p$$

$$\partial_t \mathbf{C} = \nabla^2\mathbf{A} + \kappa(\mathbf{j}_e - \mathbf{j}_p), \qquad \partial_t \mathbf{A} = \mathbf{C}, \qquad \partial_t \varphi = -\nabla\cdot\mathbf{A}$$

$$\varphi = A^o, \qquad \mathbf{j}_e \equiv \overline{\Psi}_e \gamma \Psi_e, \qquad \mathbf{j}_p \equiv \overline{\Psi}_p \gamma \Psi_p \tag{12}$$

If we set κ=0 and assume that φ and **A** are initially zero, then the equations for Ψ_e and Ψ_p are linear. In this case, both Ψ_e and Ψ_p have linear solutions (Ψ being either one):

$$\Psi(\mathbf{x},t) = \sum_{\mathbf{k}} \left[\cos(\omega_k t) - i\omega_k^{-1}\left(\beta + \alpha\cdot\mathbf{k}\right)\sin(\omega_k t)\right]\Phi(\mathbf{k})\, e^{i\,\mathbf{k}\cdot\mathbf{x}} \tag{13}$$

where $\Phi(\mathbf{k})$ is a time-independent, complex, four component column vector and $\omega_k = (k^2+1)^{1/2}$. The lowest frequency is obviously $\omega_o = 1$, with a corresponding period of $T_o = 2\pi$. Even though we will examine non-linear behavior (κ>0) and will not utilize (13) further, (13) indicates that a simulation needs to be run from t=0 to at least t=T_o.

The fields which comprise the system (12) are seen to be, using (3),

$$\begin{gathered} R_1,\ R_2,\ R_3,\ R_4,\ S_1,\ S_2,\ S_3,\ S_4 \\ \varphi,\ A_x,\ A_y,\ A_z,\ C_x,\ C_y,\ C_z \\ P_1,\ P_2,\ P_3,\ P_4,\ Q_1,\ Q_2,\ Q_3,\ Q_4 \end{gathered} \tag{14}$$

In the numerical method, these are expanded in terms of spatial Fourier series, for example,

$$R_1(\mathbf{x},t) = \sum_{\mathbf{k}} R_1(\mathbf{k},t)\, e^{i\mathbf{k}\cdot\mathbf{x}} \tag{15}$$

Thus, the few non-linear partial differential equations in (12) are transformed into many non-linear ordinary (in time) differential equations.

In addition to the equations in (12), there is also an auxiliary condition which must be satisfied:

$$-\nabla^2\varphi = \kappa(\rho_e - \rho_p) + \nabla\cdot\mathbf{C} \tag{16}$$

where

$$\rho_e = j_e^o \equiv \overline{\Psi}_e\beta\Psi_e\,, \qquad \rho_p = j_p^o \equiv \overline{\Psi}_p\beta\Psi_p. \tag{17}$$

Equation (16) arises when the Lorentz condition and the wave equation for the electric potential φ are combined. Thus, in (14) φ is not an independent dynamic variable; however, either (16) or the Lorentz gauge $\partial_t\varphi = -\nabla\cdot\mathbf{A}$ can be used to determine φ during the dynamic evolution of the system (whichever is more computationally efficient - here the Lorentz condition is used). Initially, however, (16) is always needed to determine φ.

In a spatial Fourier method, the Lorentz condition is $d\varphi(\mathbf{k})/dt + i\mathbf{k}\cdot\mathbf{A}(\mathbf{k}) = 0$, and a gauge transformation of the electromagnetic fields has the modal form $\{\mathbf{A}(\mathbf{k}), \mathbf{C}(\mathbf{k})\}\rightarrow \{\mathbf{A}(\mathbf{k}) - i\mathbf{k}\theta(\mathbf{k}), \mathbf{C}(\mathbf{k}) - i\mathbf{k}d\theta(\mathbf{k})/dt\}$. Here $\theta(\mathbf{k})$ satisfies the modal wave equation $d^2\theta(\mathbf{k})/dt^2 + k^2\theta(\mathbf{k}) = 0$. Under a gauge transformation, the modal form of the change of the quantum mecahnical wave function is $\Psi(\mathbf{k})\rightarrow \{\exp(i\theta)\Psi\}(\mathbf{k})$; *i.e.*, the modal gauge transformation is just the spatial Fourier transform of the physical space gauge transformation, *as long as all possible modes* $\mathbf{k}$ *are retained.* This last stipulation results from the observation that the spatial Fourier transform of $\exp(i\theta)$ must have an infinite number of modes, and the numerical method cannot de-alias a quadratic product where one

of the cofactors is known to contain more than the truncated set of modes. However, if invariance under only an infinitesimal gauge transformation $\Psi(\mathbf{k}) \rightarrow \{(1+ i\theta)\Psi\}(\mathbf{k})$ is required (at each numerical time-step), and θ is restricted to contain no modes outside the truncated set, then the numerical method is gauge invariant.

In the present numerical method, each field (for an NxNxN spatial grid) has approximately 0.4388 N^3 degrees-of-freedom (real and imaginary parts of independent Fourier modes). Thus each of the fields in (14) for a 32^3 grid has about 14400 degrees-of-freedom, and since there are 22 independent fields, the model system has a total of about 320,000 degrees-of-freedom. Computationally, this means that we have this many coupled, nonlinear, ordinary differential equations to solve. (Although it will not be done here, an an N=64 simulation is also be possible. This, of course, requires a correspondingly greater investment of computer resources.)

One long simulation will be presented in detail here. This was run on a Cray YMP, with a cpu time per simulation time step of about 14 seconds for N=32. The coupling constant was $\kappa = 1$ and the initial conditions were such that only R_1 S_2, P_2, and Q_1 were nonzero with $\langle R_1^2\rangle = \langle S_2^2\rangle = \langle P_2^2\rangle = \langle Q_1^2\rangle$ (*i.e.*, neither the electron nor the positron had any initial kinetic energy, linear momentum, or angular momentum). Initially, R_1 S_2, P_2, and Q_1 were described by spatial three-dimensional gaussian density distributions centered on the grid points (8,16,16), (16,8,8), (24,16,16), and (16,24,16), respectively; all had standard deviations of 8 grid spacings and were set to zero beyond one standard deviation from their respective centers. Also, at t = 0, $\mathbf{A} = \mathbf{C} = \mathbf{0}$, and φ was determined by (16). Each computational time step advanced the system Δt=0.000125 simulation time units.

During the simulation, which ran from t= 0 to 6.3 (*i.e.*, 2π), the normalization of the electron and positron wave functions was conserved to 1 part in 10^6 (thus, total charge was conserved to this accuracy, and there was no 'blow-up' [6]). The total energy given in (9) was also conserved extremely well, fluctuating no more than 0.04 % during the run.

Thus, the Noether invariants of nomalization (*i. e.*, total charge, probability, or particle number) and energy were essentially conserved during the run.

Another measure of numerical efficacy lies in behavior of the "center of inertia" **R** of the system, which should remain fixed (since the **P=0** at t=0) for both runs. Here, we define **R** as

$$\mathbf{R}(t) = \int_0^t \frac{\mathbf{P}}{E}\, dt \tag{18}$$

where **P** is the total momentum, as given by (10), and E is the total energy, as given by (9). Since the edge length of the computational 3-D volume is 2π, the percent variation is defined as $100\% \times |\mathbf{R}(t)|/2\pi$. The fluctuation in the center of inertia was less than 0.4 %, commensurate with the numerical variation in energy.

To get an appreciation of the difference between linear and non-linear evolution, consider Fiqure 1, where the linear and non-linear time dependence of the Fourier coefficients $R_1(\mathbf{k},t)$ and $S_1(\mathbf{k},t)$ for $\mathbf{k}=\mathbf{0}$ is compared (for $\mathbf{k}=\mathbf{0}$, all coefficients are real). According to (13) the linear behavior of the pair should be $R_1(\mathbf{0},t)=\cos(t)$ and $S_1(\mathbf{0},t)=-\sin(t)$ (for this figure, the amplitude has been normalized to unity). The actual trajectory of the pair is obviously different from the linear prediction; there are clearly many more frequencies present than just the single one corresponding to the linear mode. In fact, if the behavior of any coefficient is examined in a similar manner, the same behavior will be seen: a 'random walk' around the origin.

To get another view on the dynamic evolution of the model system, let us break up the total energy (9) into its constituent parts:

$$E_e = \left\langle -i\overline{\Psi}_e \gamma\cdot\nabla\, \Psi_e + \overline{\Psi}_e \Psi_e \right\rangle, \qquad E_p = \left\langle -i\overline{\Psi}_p \gamma\cdot\nabla\, \Psi_p + \overline{\Psi}_p \Psi_p \right\rangle$$
$$E_I = \left\langle -\mathbf{A}\cdot(\mathbf{j}_e - \mathbf{j}_p) \right\rangle, \qquad E_{EM} = \left\langle \tfrac{1}{2}\left(|\mathbf{E}|^2 + |\mathbf{H}|^2\right) \right\rangle \tag{19}$$

Here we have defined the "electron's energy" E_e, "positron's energy" E_p, "interaction energy" E_I, and electromagnetic energy E_{EM}. The evolution of these energies is shown in Figure 2.

Next, consider the quantities

$$\left\langle |\Psi_{e,i}|^2 \right\rangle = \left\langle R_i^2 + S_i^2 \right\rangle, \qquad \left\langle |\Psi_{p,i}|^2 \right\rangle = \left\langle P_i^2 + Q_i^2 \right\rangle, \qquad i = 1,2,3,4 \tag{20}$$

These are just the contributions each component makes to their respective normalization integral (8). Their time evolution is given in Figures 3 and 4 for the electron and positron fields, respectively.

5. Quantum Mechanical Turbulence

Let us now take up the matter of nonlinear dynamics and turbulence in this multi-mode quantum mechanical system. The parameter κ plays a role in (12) analogous to that played by the Reynolds number in fluid turbulence, *i. e.*, as these numbers tend to zero the nonlinear effects in the respective systems disappear. A characteristic of turbulent behavior is the manner in which energy (or probability) is shared nonlinearly between different modes. This is illustrated for the present simulation in Figures 5 and 6, where the wave number spectra of the electron probability density and electromagnetic energy density, respectively, at several different times are shown. (The positron spectra are very similar to the electron spectra.) (In a 32^3 run, the maximum wave number is 15.07, and thus $\log(k_{max})=1.17$). The spectra shown in Figures 5 and 6 are derived from the modal densities by finding the average over all $\mathbf{k}$ with the same magnitude $|\mathbf{k}|=k$, and multiplying this average by k^2. These "omnidirectional" spectra are, explicitly:

$$
\begin{aligned}
e(k) &= \frac{k^2}{N(k)} \sum_{|\mathbf{k}|=k} \left\{ \sum_{i=1}^{4} \left[R_i^2(\mathbf{k}) + S_i^2(\mathbf{k}) \right] \right\} \\
em(k) &= \frac{k^2}{N(k)} \sum_{|\mathbf{k}|=k} \frac{1}{2} \left\{ \sum_{i=1}^{3} \left[k^2 A_i^2(\mathbf{k}) + C_i^2(\mathbf{k}) \right] \right\} \\
p(k) &= \frac{k^2}{N(k)} \sum_{|\mathbf{k}|=k} \left\{ \sum_{i=1}^{4} \left[P_i^2(\mathbf{k}) + Q_i^2(\mathbf{k}) \right] \right\}
\end{aligned}
\tag{21}
$$

Here, N(k) is the number of terms in the summation over $\mathbf{k}$ such that $|\mathbf{k}|=k$. (The values of $P_e(k)$ and $P_{em}(k)$ shown in Figures 5 and 6, respectively, are smoothed by averaging over nearest neighbors.)

The shape of the spectra at t = 0 is the initial spectra (in a linear run, where $\kappa=0$, these spectra do not change shape at all with time). As is seen in Figures 5 and 6, there was a considerable amount of energy and probability transfer between the different modes; in fact, all the spectra appear to be converging to equilibria.

It should be possible to predict these spectra *a priori* as is done, for example, in ideal three-dimensional magneto-fluid turbulence [15], since the system of equations (12) satisfy all the criteria necessary for 'absoulte equibrium ensemble' theory to apply [16]. In particular, a partition function involving the numerical invariants of the model system is determined and used to construct canonical ensemble predictions, for example, of turbulent energy spectra [17]. (This procedure has a close analogy to work in lattice field theory, where a partition function involving a Eucidean action is sought [18]; remember though, that the model underlying the simulation here is a continuum model, while that of lattice gauge theory is not.) However, in non-dissipative fluid turbulence, the invariants are quadratic sums, while the situation here is more complicated since, for example, the interaction energy E_I is cubic in nature, and the relation (16) between the potential and the dynamical fields introduces a term quartic in the wave functions into the energy expression. Developing this possibility will be deferred.

In order to actually "see" the interaction, consider Figure 7. This figure indicates the relative values of the electron's 3-D probability density $|\Psi_e(\mathbf{x})|^2$, the electromagnetic 3-D energy density $E_{em}(\mathbf{x})$, and the positron's 3-D probability density $|\Psi_p(\mathbf{x})|^2$, summed in the z-direction and projected onto the x-y plane for equally spaced times during the run.

Figures 5, 6, and 7 indicate a relative change in size of the various physical fields with time, a change which can be quantified by defining wave numbers K_{ep} and K_{em} :

$$K_{ep}^2 = \frac{\sum_k k^2[P_e(k)+P_p(k)]}{\sum_k [P_e(k)+P_p(k)]}, \qquad K_{em}^2 = \frac{\sum_k k^2 P_{em}(k)}{\sum_k P_{em}(k)} \tag{22}$$

where the P_i (i=*e,p,em*) are given in (21). The time evolution of these root-mean-square (rms) wave numbers are shown in Figure 8.

Although the spectra shown in Figures 5 and 6 and defined by (21), and the rms wave numbers shown in Figure 8 and defined by (22), are determined by averaging over

all directions, the turbulence which is simulated is not in fact isotropic. We can define a measure of anisotropy in the x-direction as follows:

$$M_x = N_{xyz} = \frac{\left\langle |\partial_x \Psi|^2 \right\rangle - \frac{1}{2}\left[\left\langle |\partial_y \Psi|^2 \right\rangle + \left\langle |\partial_z \Psi|^2 \right\rangle\right]}{\left\langle |\partial_x \Psi|^2 \right\rangle + \left\langle |\partial_y \Psi|^2 \right\rangle + \left\langle |\partial_z \Psi|^2 \right\rangle} \tag{23}$$

Then measures of anisotropy in the y- and z-directions are $M_y=N_{yzx}$ and $M_z=N_{zxy}$, respectively, and satisfy $M_x+M_y+M_z=0$ (these measures are similar to those used in fluid turbulence work [19]). The quantity Ψ can be either the electron or positron wave function or the complex electromagnetic vector $\mathbf{A}+i\mathbf{C}$. The quantities M_x, M_y, and M_z change with time; in Figure 9, the evolution of these quantities for the electron ($\Psi=\Psi_e$) is shown. Measures of the positron and electromagnetic anisotropy behaved very similarly.

The observed anisotropy occurs because we have a mixture of "charged fluids". At t=0 the electron and positron densities are separated, more or less, along the x-axis and are initially motionless. Since the initial densities are composed of spherical distributions, and have no motion, we have $M_x=M_y=M_z=0$ at t=0, according to (23), for the elctron and positron (the electromagnetic field has a slight initial anisotropy). However, as the particles are electrically attracted, they begin to "move" in response to one another, and this is reflected by gradients in the x-direction increasing more quickly than gradients in the other two directions. Hence, the anisotropy is contained in the initial conditions and manifests itself in the direction of "plasma oscillations". Thus we have homogeneous (because the nonlinear dynamics occurs in a periodic cell in space) but anisotropic turbulent phenomena.

6. Conclusion

In this article, the numerical simulation of a nonlinear quantum mechanical lepton-photon interaction has been described. This simulation was performed using a truncated spatial Fourier method to march the classical system equations forward in time. It was seen that the interaction was highly nonlinear, and that the time-evolution of the wave functions could be described as 'turbulent', when the interaction was nominally "strong" (*i.e.*, κ=1). Conversely, if setting κ=1 results in the rapid transfer of probability and energy between spatial modes, then this sets the natural 'equilibrium' interaction scale length as $L_o = \alpha^{1/3}\lambda_c$ (= 0.47 pm for electrons). That these closely interacting fermionic wave functions quickly approached a multi-mode, dynamic equilibrium, is indicated by the various Figures.

Natural extensions of the present work are the following. First, propagating electromagnetic fields can be introduced into the initial conditions to examine their effects on the behavior of the system. Second higher resolution (*e. g.*, 64^3) runs can be performed, perhaps on a massively parallel processing system. Third, a statistical theory based on a classical partition function involving system invariants can be developed. Fourth, the work can be extended to encompass nonabelian gauge fields. This last possibility is an intriguing one as it could provide a non-perturbative method for studying few-body interactions in such quantum systems as the quark-gluon plasma.

The classical results described here pertain only to a quantum mechanical system of interacting single particles. A multiparticle treatment must, of course, be based on quantum field theory, as has been done, for example, by Bialynicki-Birula, *et al.* [7]. The main intent here, however, was to demonstrate highly nonlinear behavior in a quantum mechanical system and to present a numerical method for observing that behavior. In so doing, we have shown that a microscopic quantum mechanical system and macroscopic classical system (such as a fluid) have a common mechanism, *i.e.*, a parameteric non-linear coupling, which can induce a host of interesting phenomena (such as turbulence) into the dynamical behavior of either system.

References

[1] S. A. Orszag and G. S. Patterson, Phys. Rev. Lett., 28 (1972) 76-79.

[2] E. N. Lorenz, J. Atmos, Sci., 20 (1963) 130-141.

[3] J. R. Wilson, Ap. J., 173 (1972) 431-438.

[4] E. A. McCullough and R. E. Wyatt, J. Chem. Phys., 51 (1969) 1253-1254; 54 (1971) 3578-3591; 54 (1971) 3592-3600.

[5] A. Alvarez, Phys. Rev. D, 31, (1985) 2701-2703.

[6] A. Alvarez and A. F. Rañada, Phys. Rev. D, 38 (1988) 3330-3333.

[7] I. Bialynicki-Birula, P. Górnicki, and J. Rafelski, Phys. Rev. D, 44 (1991) 1825-1835.

[8] J. D. Bjorken and S. D. Drell, Relativistic Quantum Mechanics (McGraw-Hill, New York, 1964), pp. 281-284.

[9] M. Demianski, Relativistic Astrophysics (Pergamon, Oxford, 1985), pp. 131-141.

[10] N. N. Bogoliubov and D. V. Shirkov, Introduction to the Theory of Quantized Fields, 3rd edition (Wiley, New York, 1980), Chp. 1.

[11] C. Canuto, M. Y. Hussaini, A Quarteroni, and T. A. Zang, Spectral Methods in Fluid Dynamics (Springer-Verlag, New York, 1988).

[12] G. S. Patterson and S. A. Orszag, Phys. Fluids, 14 (1971) 2538-2541.

[13] J. Gazdag, J. Comp. Phys., 20 (1976) 196-207.

[14] C. Leforestier, et al., J. Comp. Phys., 94 (1991) 59-80.

[15] U. Frisch, A. Pouquet, J. Leorat, and A. Mazure, J. Fluid Mech., 68 (1975), 769-778.

[16] T. D. Lee, Q. Appl. Math., 10 (1952) 69-74.

[17] J. V. Shebalin, Physica D, 37 (1989) 173-191.

[18] I. J. R. Aitchison and A. J. G. Hey, Gauge Theories in Particle Physics, 2nd edition (Adam Hilger, Bristol, 1989), pp. 492-505.

[19] C. G. Speziale, S. Sarkar, and T. B. Gatski, J. Fluid Mech., 227 (1991), 245-272.

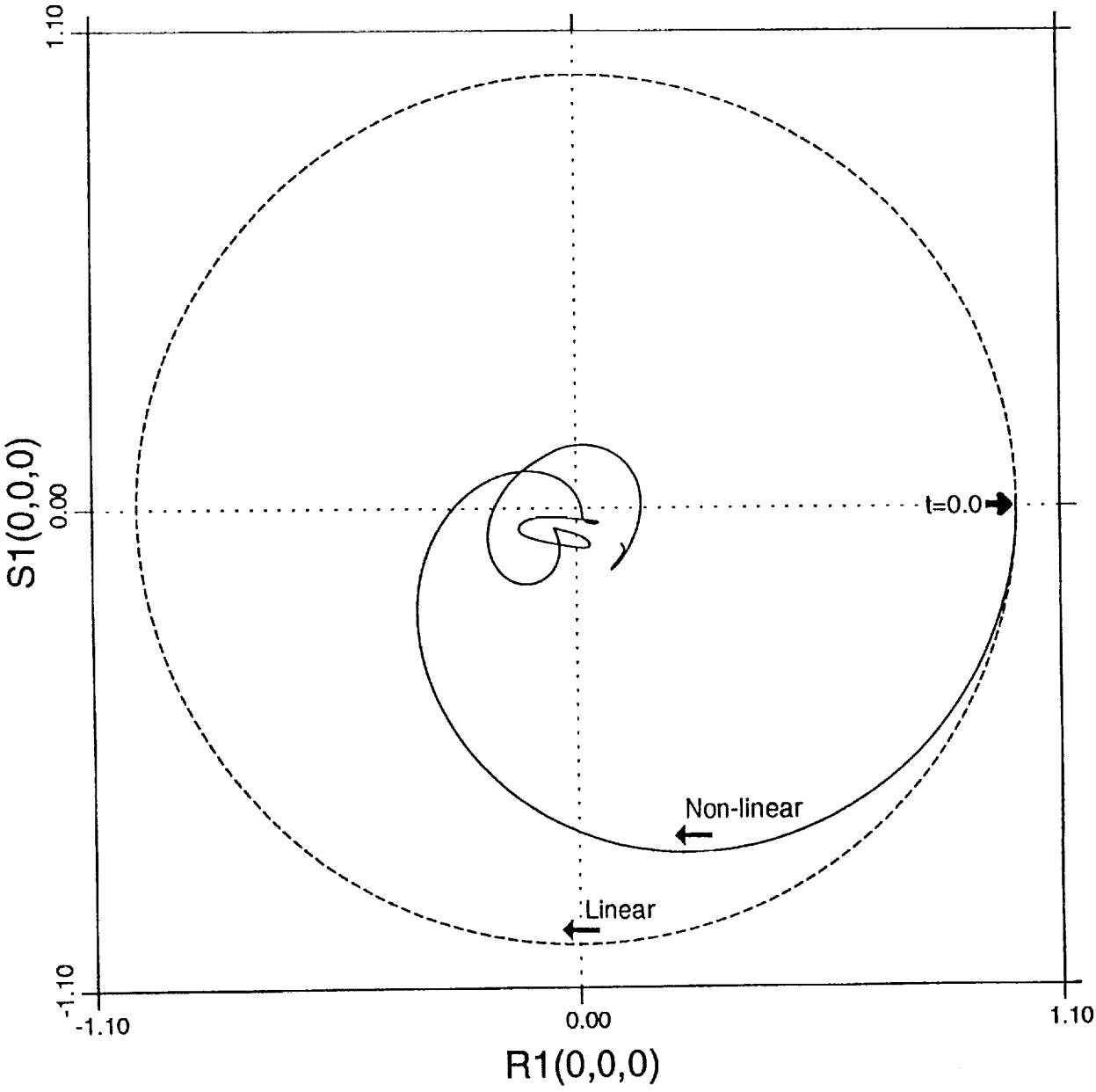

Figure 1. Comparison of linear and nonlinear evolution of a pair of Fourier coefficients.

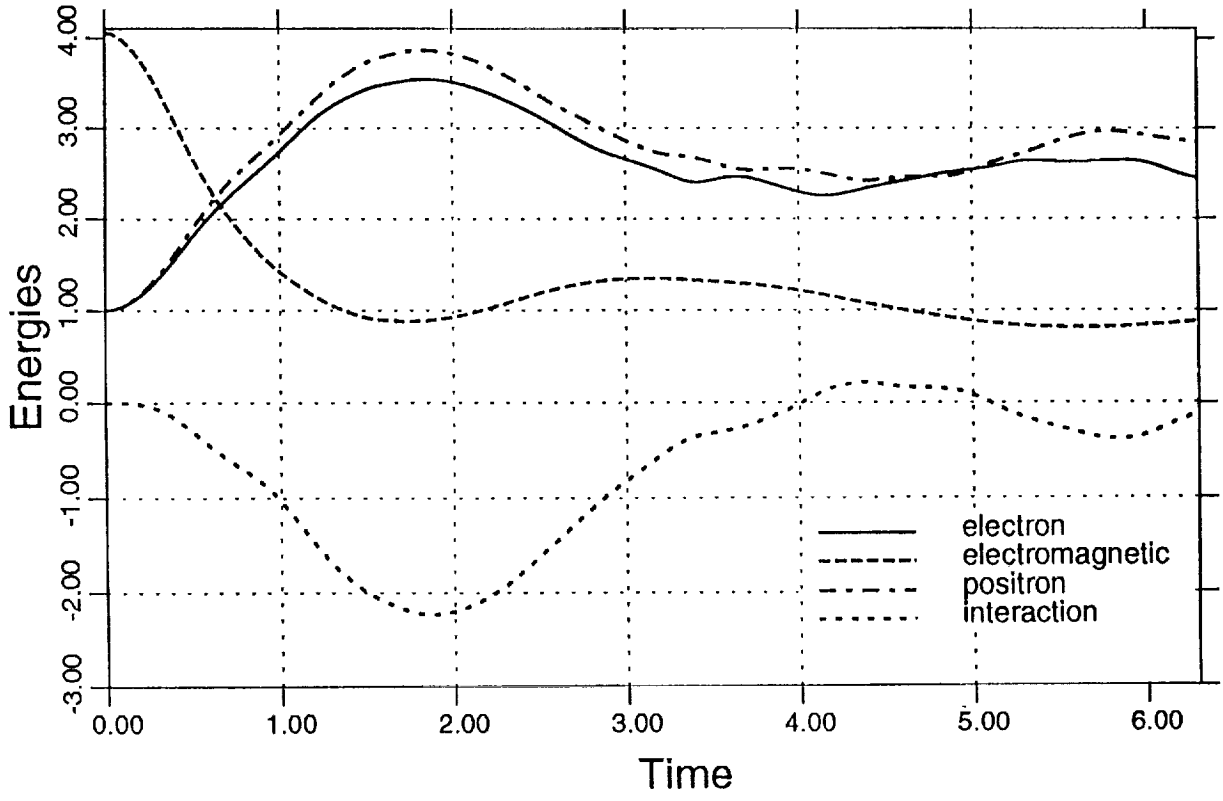

Figure 2. Time variation of electron, positron, electromagnetic, and interaction energies.

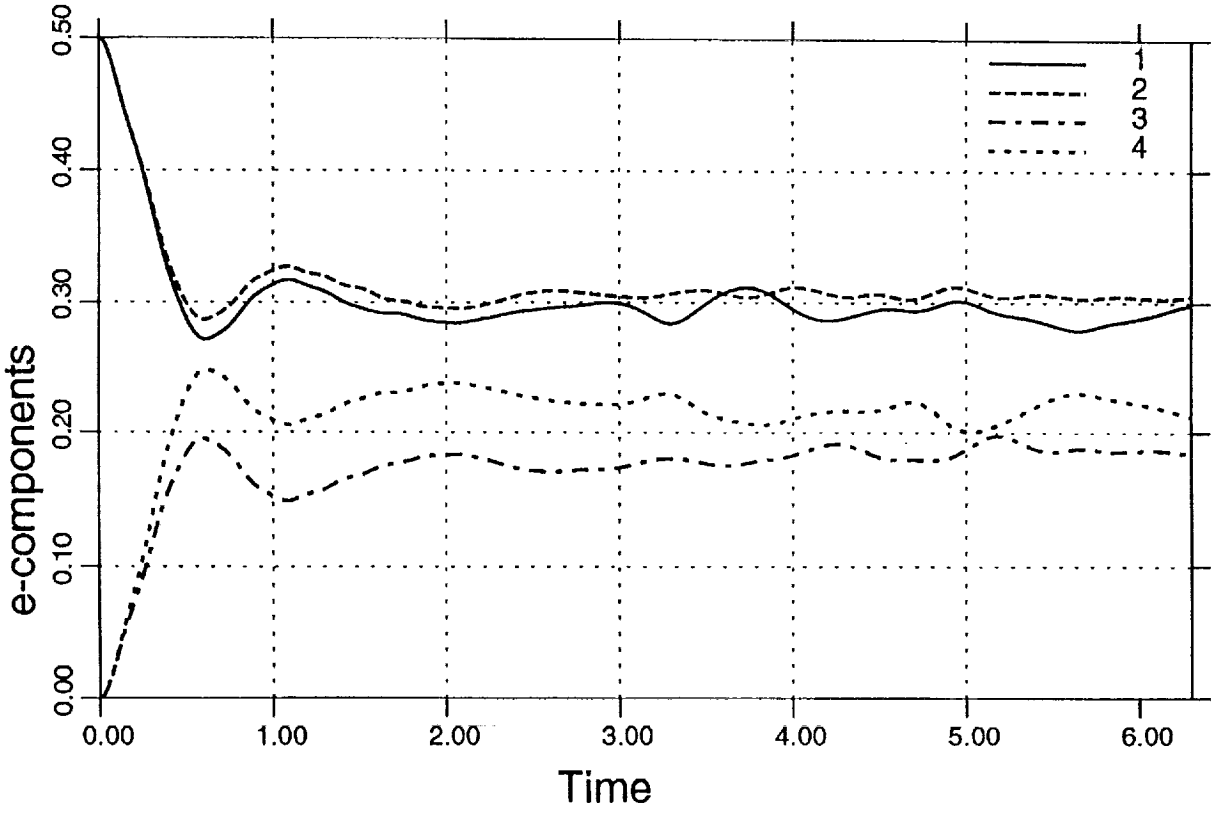

Figure 3. Electron components ($<|\Psi_{e,i}|^2>$, i=1,2,3,4) versus time.

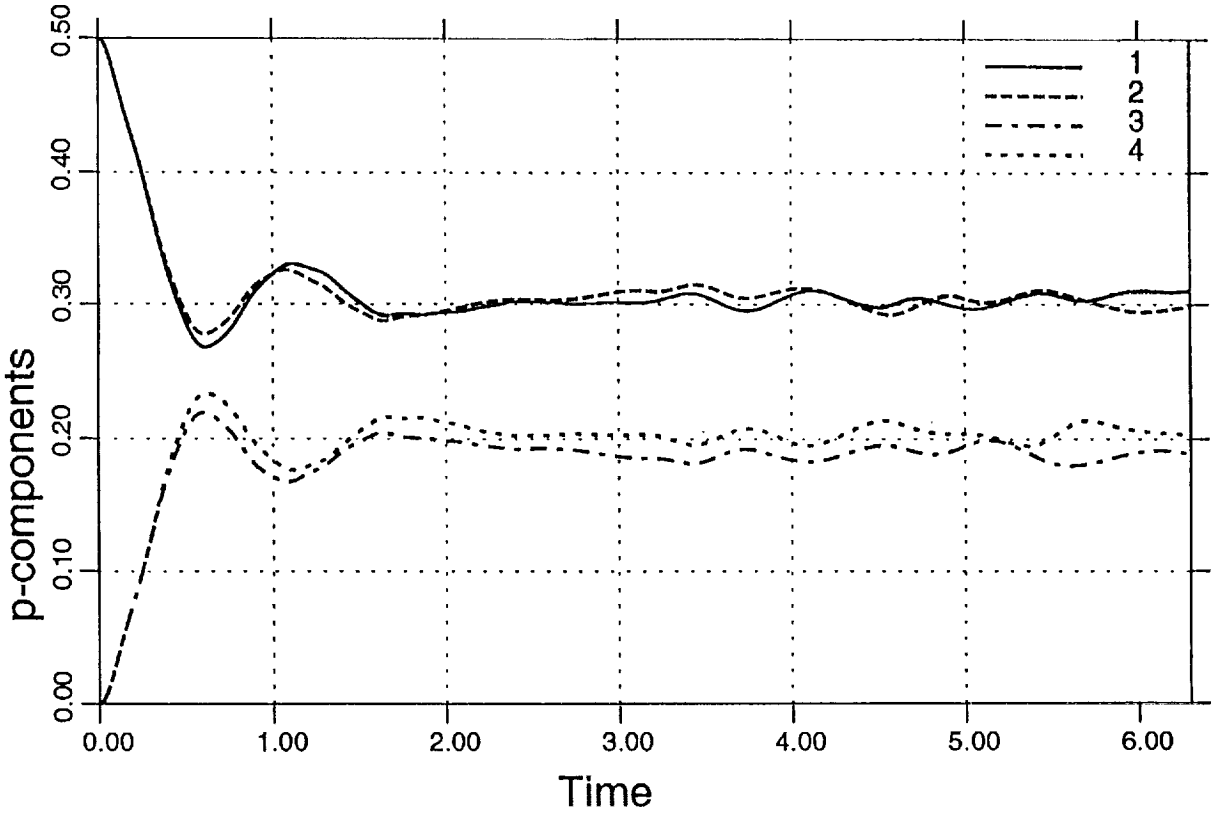

Figure 4. Positron components ($\langle|\Psi_{p,i}|^2\rangle$, i=1,2,3,4) versus time.

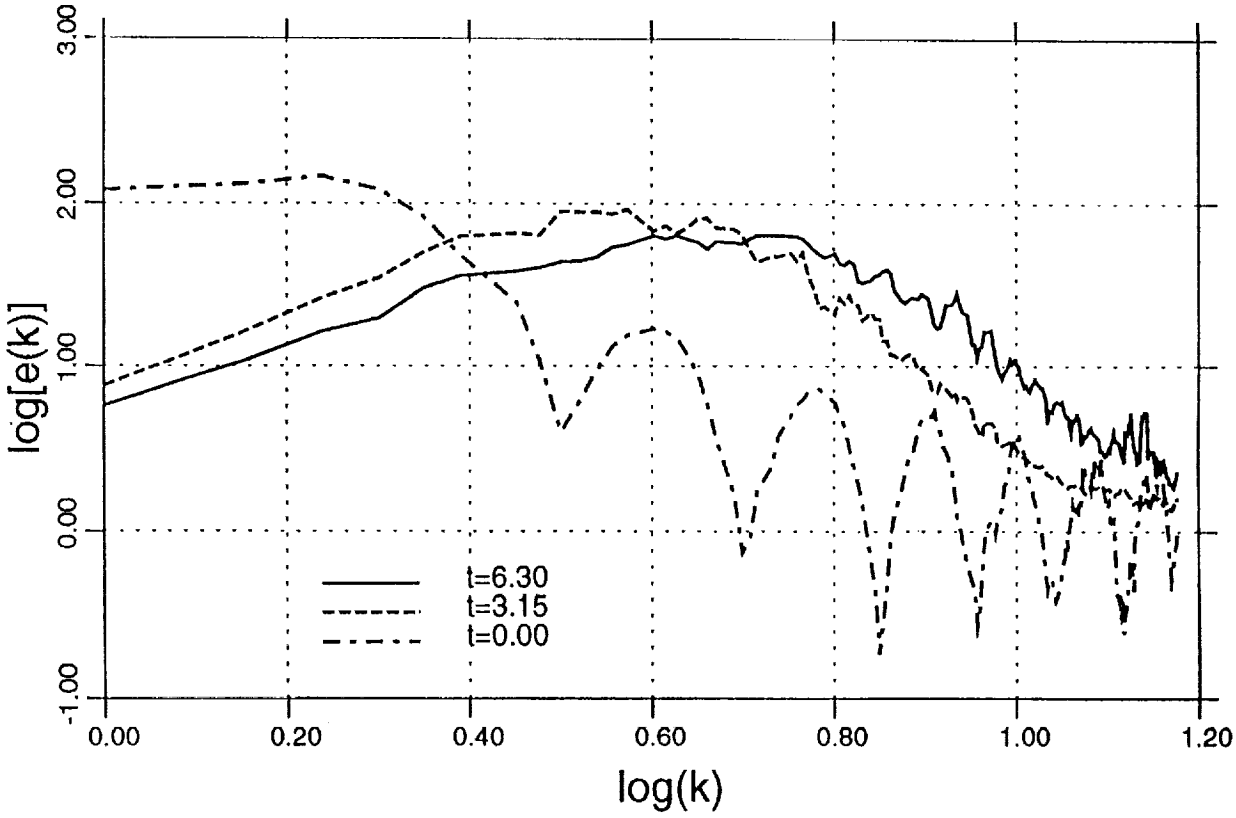

Figure 5. Electron omnidirectional density spectra at various times.

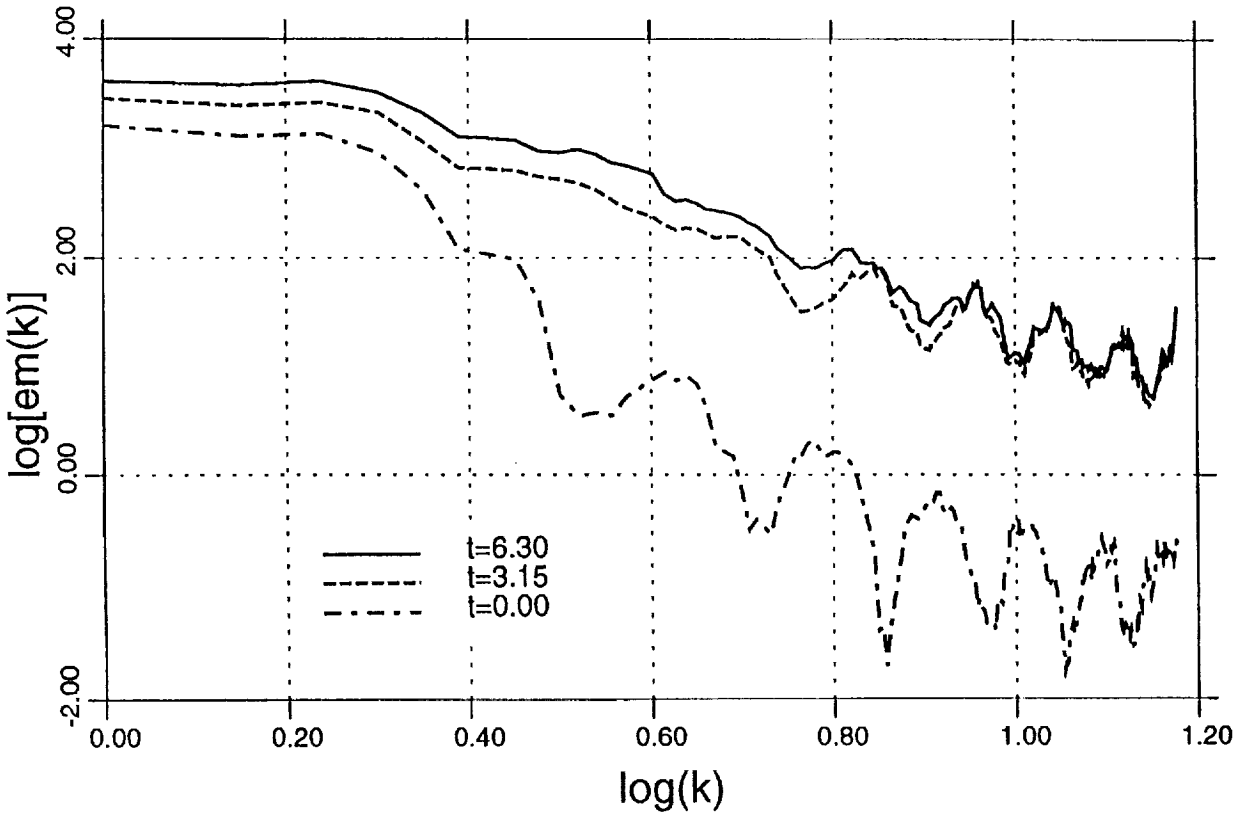

Figure 6. Electromagnetic omnidirectional spectra at various times.

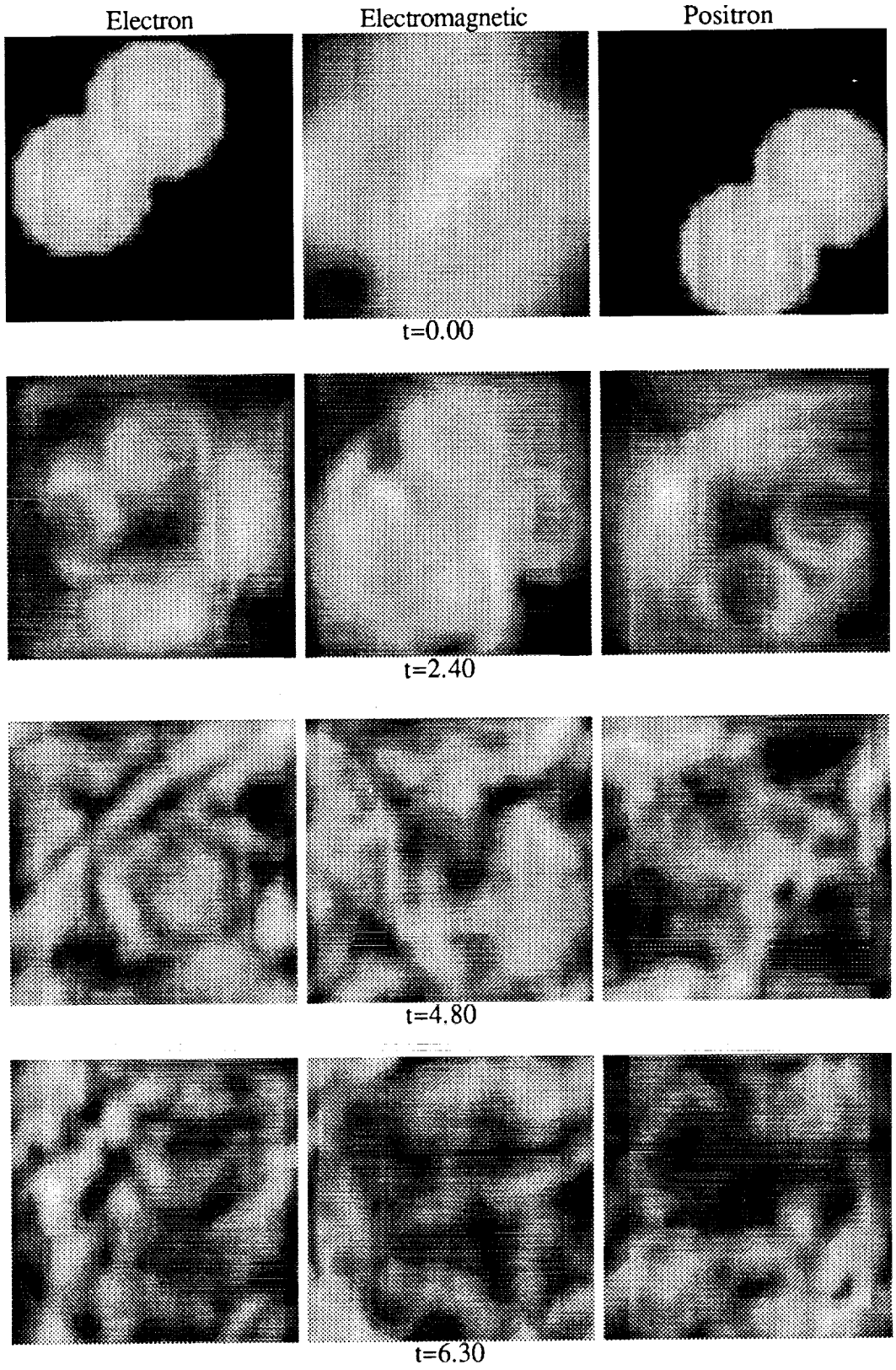

Figure 7. Spatial densities of electron and positron probability, and electromagnetic energy, averaged over z and projected onto x-y plane, at various times (black-lowest to white-highest).

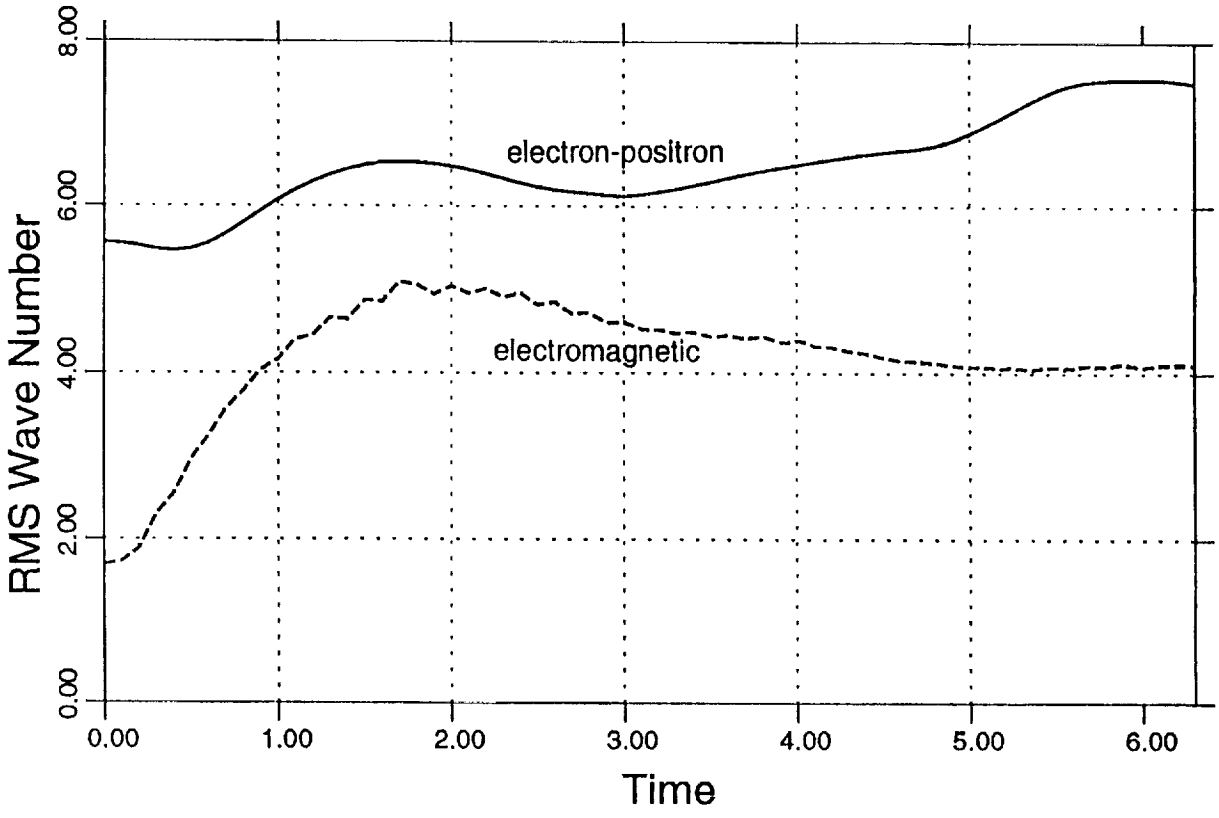

Figure 8. RMS wave numbers for the combined electron-positron spectra (K_{ep}) and for the electromagnetic spectra (K_{em}).

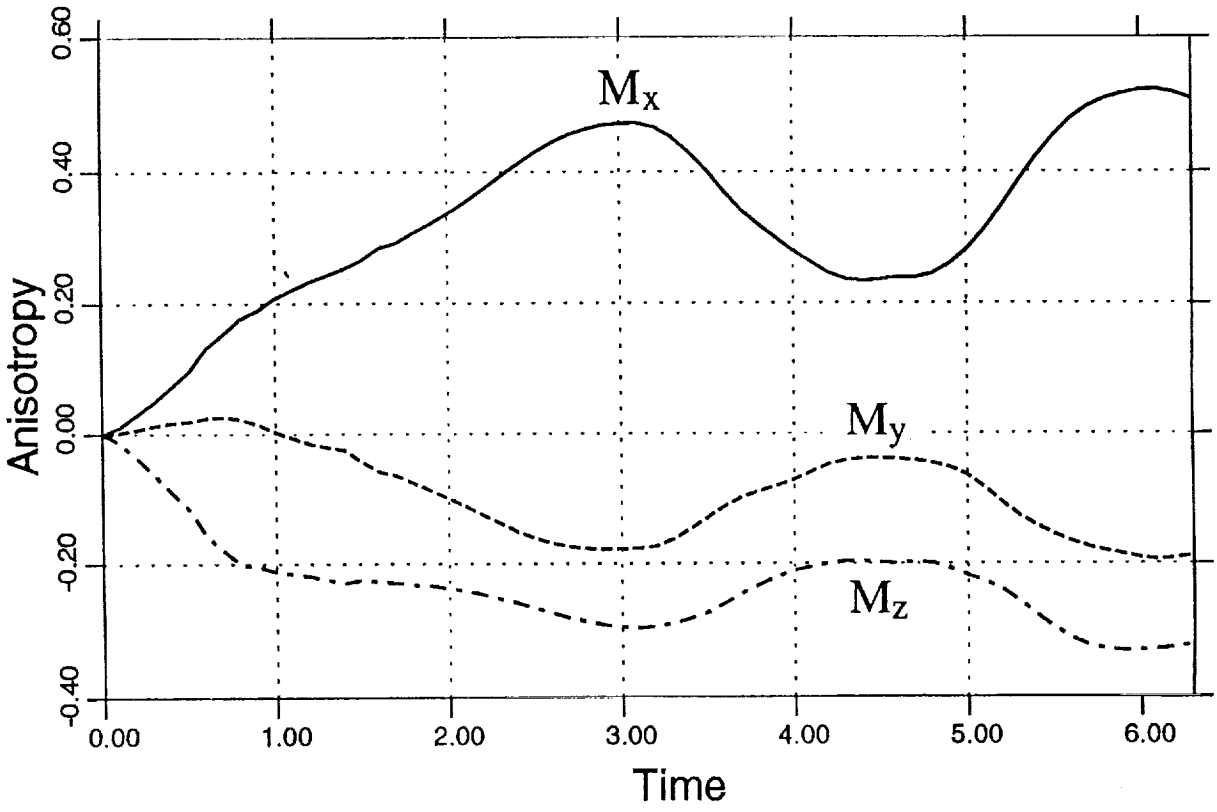

Figure 9. Measures of anisotropy for the turbulent evolution of the electron wave function..

REPORT DOCUMENTATION PAGE

Form Approved
OMB No. 0704-0188

1. AGENCY USE ONLY (Leave blank)	2. REPORT DATE	3. REPORT TYPE AND DATES COVERED
	October 1992	Technical Memorandum

4. TITLE AND SUBTITLE
HOMOGENEOUS QUANTUM ELECTRODYNAMIC TURBULENCE

5. FUNDING NUMBERS
WU 505-90-52-01

6. AUTHOR(S)
John V. Shebalin

7. PERFORMING ORGANIZATION NAME(S) AND ADDRESS(ES)
NASA Langley Research Center
Hampton, VA 23681-0001 and
Institute for Computer Applications in Science
and Engineering
NASA Langley Research Center, Hampton, VA 23681-0001

8. PERFORMING ORGANIZATION REPORT NUMBER

9. SPONSORING/MONITORING AGENCY NAME(S) AND ADDRESS(ES)
National Aeronautics and Space Administration
Washington, DC 20546-0001

10. SPONSORING/MONITORING AGENCY REPORT NUMBER
NASA TM-107686
ICASE Report No. 92-50

11. SUPPLEMENTARY NOTES
Submitted to Physica D

John V. Shebalin: Langley Research Center, Hampton, VA.
Author is currently in residence as a visiting scientist at the Institute for Computer Applications in Science and Engineering.

12a. DISTRIBUTION/AVAILABILITY STATEMENT
Unclassified - Unlimited
Subject Category 73

12b. DISTRIBUTION CODE

13. ABSTRACT *(Maximum 200 words)*

The electromagnetic field equations and Dirac equations for oppositely charged wave functions are numerically time-integrated using a spatial Fourier method. The numerical approach used, a spectral transform technique, is based on a continuum representation of physical space. The coupled classical field equations contain a dimensionless parameter which sets the strength of the nonlinear interaction (as the parameter increases, interaction volume decreases). For a parameter value of unity, highly nonlinear behavior in the time-evolution of an individual wave function, analogous to ideal fluid turbulence, is observed. In the truncated Fourier representation which is numerically implemented here, the quantum turbulence is homogenous but anisotropic and manifests itself in the nonlinear evolution of equilibrium modal spatial spectra for the probability density of each particle and also for the electromagnetic energy density. The results show that nonlinearly interacting fermionic wave functions quickly approach a multi-mode, dynamic equilibrium state, and that this state can be determined by numerical means.

14. SUBJECT TERMS	15. NUMBER OF PAGES
homogeneous turbulence; quantum electrodynamics	28
	16. PRICE CODE: A03

17. SECURITY CLASSIFICATION OF REPORT	18. SECURITY CLASSIFICATION OF THIS PAGE	19. SECURITY CLASSIFICATION OF ABSTRACT	20. LIMITATION OF ABSTRACT
Unclassified	Unclassified		